International Journal for Modern Trends in Science and Technology
Volume 12, Issue 05, pages 466-476
ISSN: 2455-3778 online
Available online at: http://www.ijmtst.com/vol12issue05.html
DOI: https://doi.org/10.5281/zenodo.20568152

Adaptive ANN-Controlled DC-Coupled Fast EV Charging Station with Wind–Solar Hybrid Energy Storage System

Dr. J. Srinu Naick | P. Hemalatha | B. Manikanteswara | A. Alameen | P. Tharun

Department of Electrical and Electronics Engineering, Chadalawada Ramanamma Engineering College, Tirupati, Andhra Pradesh, India.

To Cite this Article
Dr. J. Srinu Naick, P. Hemalatha, B. Manikanteswara, A. Alameen & P. Tharun (2026). Adaptive ANN-Controlled DC-Coupled Fast EV Charging Station with Wind–Solar Hybrid Energy Storage System, International Journal for Modern Trends in Science and Technology, 12(05), 466-476. https://doi.org/10.5281/zenodo.20568152

Article Info
Received: 07 May 2026; Revised: 26 May 2026; Accepted: 30 May 2026.

KEYWORDS

Adaptive control,
Artificial Neural Network (ANN),
DC-coupled EV charging station,
Renewable energy integration,
Solar–wind hybrid system,
Battery energy storage system (BESS),
Bidirectional power flow,
DC bus voltage regulation,
Fast EV charging,
Smart grid support

ABSTRACT

This paper presents an adaptive artificial neural network (ANN)-controlled hierarchical strategy for a dc-coupled fast electric vehicle (EV) charging station integrated with a hybrid renewable energy system. The proposed system combines solar photovoltaic (PV), wind energy, and battery energy storage to enhance power reliability and reduce dependency on the utility grid. Unlike conventional approaches that rely on proportional–integral (PI) controllers, the proposed method employs an adaptive ANN-based controller to regulate the dc-bus voltage and dynamically coordinate power flow among multiple energy sources, EV loads, and the grid. The integration of wind energy alongside solar generation improves system reliability by compensating for the intermittency of solar power, while the battery storage system ensures energy balance and supports continuous operation under varying conditions. The ANN-based control strategy offers superior adaptability and fast dynamic response, enabling effective handling of uncertainties such as fluctuations in renewable generation, changes in EV charging demand, and variations in grid conditions. The proposed system supports bidirectional power flow, facilitating both grid-to-vehicle (G2V) and vehicle-to-grid (V2G) operations, along with grid-supportive services such as voltage regulation and stability enhancement. The hierarchical control framework ensures optimal utilization of available renewable energy while minimizing grid power consumption. Simulation results demonstrate that the proposed ANN-controlled system achieves improved dc-bus voltage regulation, enhanced stability, reduced grid dependency, and better overall performance compared to conventional PI-controlled EV charging systems. The proposed approach provides a robust and intelligent solution for next-generation fast EV charging infrastructure.

1. Introduction

The rapid growth of electric vehicles (EVs) has become a key component in the global transition toward sustainable transportation and reduced carbon emissions. Governments and industries worldwide are promoting EV adoption to mitigate environmental concerns associated with conventional fossil-fuel-based vehicles and to achieve long-term energy sustainability goals [1]. As EV penetration continues to increase, the development of efficient and reliable charging infrastructure has become a critical requirement for supporting large-scale transportation electrification [2]. Among various charging technologies, fast EV charging stations have gained significant attention because they can substantially reduce charging time and improve user convenience. However, the high-power demand associated with fast charging can impose considerable stress on power distribution networks, leading to voltage fluctuations, increased peak demand, and reduced grid stability [3]. To address these challenges, renewable-energy-integrated charging stations have emerged as a promising solution. By incorporating local renewable generation, EV charging stations can reduce dependence on utility grids while improving environmental sustainability [4]. Solar photovoltaic (PV) systems are among the most widely adopted renewable energy sources due to their modularity, low maintenance requirements, and declining installation costs [5]. Nevertheless, PV generation is highly dependent on solar irradiance and weather conditions, resulting in intermittent power output that can affect charging station reliability [6]. Consequently, relying solely on solar energy is often insufficient to ensure continuous operation of fast EV charging infrastructure. Wind energy represents another important renewable resource that can complement solar generation due to its different generation profile. In many locations, wind energy is available during periods of low solar irradiance, thereby providing a more balanced and reliable renewable power supply [7]. The integration of wind and solar resources into a hybrid renewable energy system can significantly improve energy availability, reduce power fluctuations, and enhance the overall reliability of EV charging stations [8]. Such hybrid systems have attracted considerable interest in recent years because of their ability to maximize renewable energy utilization and support sustainable transportation systems. Energy storage systems play a crucial role in renewable-integrated charging stations by compensating for the intermittent nature of renewable energy sources and maintaining power balance between generation and demand [9]. Battery Energy Storage Systems (BESS) are widely used because of their high energy density and capability to store excess renewable energy for later use [10]. During periods of insufficient renewable generation or sudden increases in charging demand, stored energy can be supplied to maintain continuous operation and reduce dependency on the utility grid. Therefore, the integration of battery storage enhances system flexibility, reliability, and power quality [11]. Recently, DC-coupled charging station architectures have gained popularity due to their higher efficiency and reduced power conversion stages compared with traditional AC-coupled systems [12]. In a DC-coupled configuration, renewable energy sources, battery storage units, and EV charging loads are connected through a common DC bus. This arrangement minimizes conversion losses, simplifies power management, and facilitates the integration of multiple energy resources [13]. Moreover, DC-coupled systems are particularly suitable for fast charging applications because they can directly supply high-power DC energy to EV batteries without multiple conversion processes [14]. The operation of renewable-integrated EV charging stations requires advanced control strategies capable of coordinating multiple energy sources while maintaining DC-bus stability. Conventional control approaches commonly employ Proportional–Integral (PI) controllers for voltage regulation and power flow management [15]. Although PI controllers are simple and widely used, their performance often deteriorates under nonlinear operating conditions, renewable generation fluctuations, and rapidly varying EV charging demands [16]. Fixed controller parameters may not provide satisfactory dynamic performance when system operating conditions change significantly. To overcome these limitations, intelligent control techniques based on Artificial Intelligence (AI) have attracted increasing attention. Among these techniques, Artificial Neural Networks (ANNs) have demonstrated significant potential for power system control applications due to their ability to model nonlinear relationships, learn system dynamics, and adapt to changing operating conditions [17]. ANN-based controllers can process

multiple input variables simultaneously and generate appropriate control actions without requiring an accurate mathematical model of the system. As a result, they offer improved robustness, adaptability, and disturbance rejection capability compared with conventional control methods [18]. In EV charging applications, ANN controllers have been successfully applied for energy management, power flow coordination, state-of-charge estimation, and renewable energy forecasting. Their ability to handle uncertainty and nonlinear system behavior makes them particularly suitable for renewable-integrated charging stations where generation and load conditions continuously vary [19]. Furthermore, ANN-based control strategies can support bidirectional power flow operations, including Grid-to-Vehicle (G2V) and Vehicle-to-Grid (V2G) modes, thereby enhancing grid support capability and improving overall energy utilization [20]. Motivated by these challenges and opportunities, this paper proposes an adaptive ANN-controlled DC-coupled fast EV charging station integrated with a hybrid wind–solar energy system and battery energy storage. The proposed hierarchical control framework dynamically coordinates power flow among renewable energy sources, battery storage, EV charging loads, and the utility grid while maintaining stable DC-bus voltage. The integration of wind and solar resources improves renewable energy utilization and operational reliability, whereas the ANN-based controller enhances dynamic response and adaptability under varying operating conditions. Simulation results demonstrate that the proposed system achieves superior DC-bus voltage regulation, improved stability, reduced grid dependency, and enhanced overall performance compared with conventional PI-controlled charging stations.

2. System Configuration

The proposed system is a DC-coupled fast EV charging station integrated with a solar PV system, wind energy conversion system (WECS), battery energy storage system (BESS), and utility grid. All components are connected through a common DC bus, which acts as the central power exchange platform. The PV array and wind generation unit supply renewable power to the DC bus through appropriate power electronic converters, while the battery storage system stores excess energy and provides backup support during power deficits. A bidirectional grid-connected converter enables power exchange between the charging station and the utility grid, supporting both Grid-to-Vehicle (G2V) and Vehicle-to-Grid (V2G) operations. Fast EV charging loads are connected to the DC bus and receive power from the available energy sources. An adaptive ANN-based controller continuously regulates the DC-bus voltage and coordinates power flow among the renewable sources, battery storage, EV chargers, and grid to ensure stable, efficient, and reliable system operation.

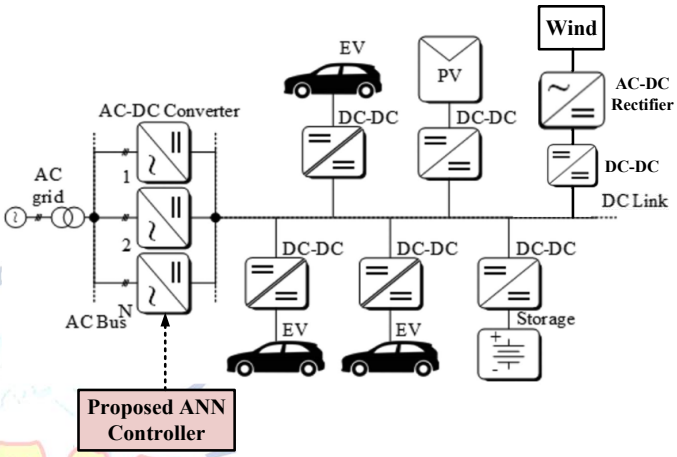

Fig. 1 Proposed DC link-coupled FEVC infrastructure

3. Configuration and Design of the Proposed System

A. Design of Solar PV Boost Converter with P&O MPPT Configuration

The solar photovoltaic (PV) system serves as one of the primary renewable energy sources in the proposed DC-coupled fast EV charging station. Since the output characteristics of the PV array are highly dependent on solar irradiance and temperature, the generated voltage and power continuously vary with environmental conditions. Therefore, a DC–DC boost converter integrated with a Perturb and Observe (P&O) Maximum Power Point Tracking (MPPT) controller is employed to ensure maximum energy extraction from the PV array and efficient utilization of solar energy.

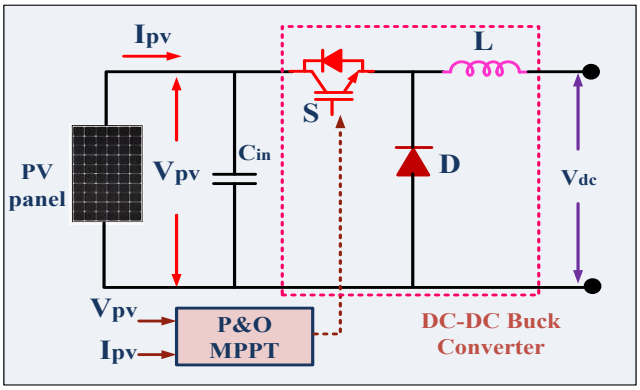

Fig. 2 solar PV P&O MPPT DC-DC Buck converter

The equivalent output current of the PV array can be represented by

$$I_{pv} = I_{Ph} - I_0\left[\exp\left(\frac{q(V_{pv}+I_{pv}R_S)}{AkT}\right) - 1\right] - \frac{V_{pv}+I_{pv}R_S}{R_{sh}} \quad (1)$$

where IPV is the PV output current, Iph is the photocurrent generated by solar irradiation, Is is the reverse saturation current of the diode, Rs and Rsh are the series and shunt resistances, respectively, q is the electron charge, k is the Boltzmann constant, T is the cell temperature, and A is the diode ideality factor.

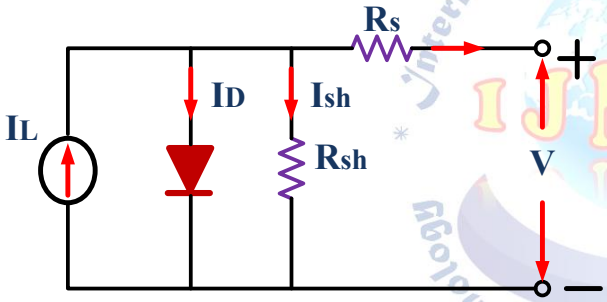

Fig. 3 equivalent model of PV solar.

The output power generated by the PV array is expressed as

$$P_{pv} = V_{pv}I_{pv} \quad (2)$$

where VPV and IPV represent the PV output voltage and current, respectively. The maximum power point (MPP) of the PV array occurs when

$$\frac{dP_{PV}}{dV_{PV}} = 0 \quad (3)$$

At this operating point, the PV system delivers the maximum available power under a given irradiance and temperature condition.

To interface the PV array with the DC bus, a boost converter is employed. The boost converter increases the relatively low PV voltage to the required DC-bus voltage level suitable for EV charging applications. The converter consists of an input inductor L, controlled switch SSS, diode D, and output capacitor C. During the ON state of the switch, energy is stored in the inductor. During the OFF state, the stored energy is transferred to the load through the diode, resulting in a higher output voltage.

The voltage conversion ratio of the boost converter is given by

$$V_{dc} = \frac{V_{PV}}{1-D} \quad (4)$$

where Vdc is the DC-bus voltage and D is the duty cycle of the converter switch. The duty cycle required to achieve the desired output voltage is calculated as

$$D = 1 - \frac{V_{PV}}{V_{dc}} \quad (5)$$

The inductor value for continuous conduction mode operation is determined by

$$L = \frac{V_{PV}\cdot D}{f_S\cdot \Delta I_L} \quad (6)$$

where fs is the switching frequency and ΔIL is the allowable inductor current ripple.

Similarly, the output capacitor is selected using

$$C = \frac{I_o\cdot D}{f_S\cdot \Delta V_o} \quad (7)$$

where Io is the output current and ΔVo is the permissible output voltage ripple.

To ensure maximum power extraction from the PV array, the Perturb and Observe (P&O) MPPT algorithm is implemented. The algorithm continuously measures the PV voltage and current and calculates the instantaneous power as

$$P(k) = V(k)\cdot I(k) \quad (8)$$

The change in power and voltage between two consecutive sampling instants are computed as

$$\Delta P = P(k) - P(k-1) \quad (9)$$

$$\Delta V = V(k) - V(k-1) \quad (10)$$

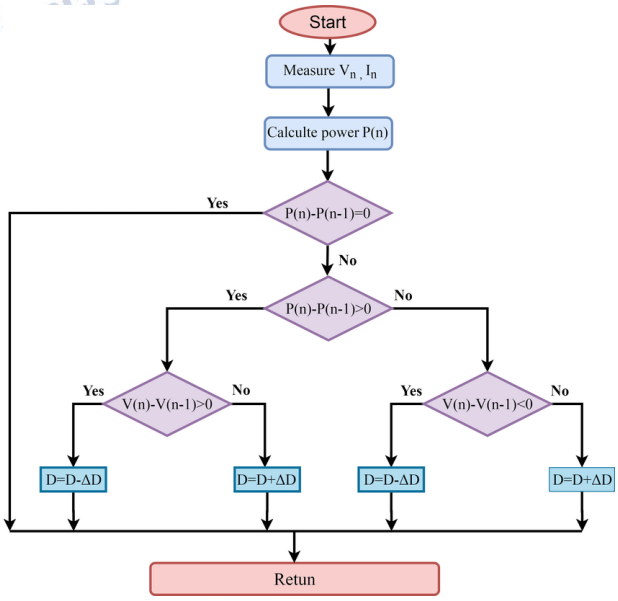

Fig.4 flow chart of P&O MPPT algorithm

Based on the values of ΔP\Delta PΔP and ΔV\Delta VΔV, the controller determines whether the operating

point is moving toward or away from the maximum power point. If the perturbation results in an increase in power, the controller continues perturbing in the same direction. Conversely, if the power decreases, the perturbation direction is reversed. This iterative process continues until the operating point reaches the maximum power point.

The output of the P&O MPPT controller generates the reference duty cycle for the boost converter, thereby ensuring that the PV array operates at its optimal power point under varying environmental conditions. Consequently, the proposed PV boost converter with P&O MPPT configuration enhances solar energy utilization, improves DC-bus voltage support, reduces dependence on the utility grid, and contributes to the reliable operation of the adaptive ANN-controlled fast EV charging station.

B. Modeling and Designing of a Bidirectional Buck-Boost Converter

a. Introduction and System Overview

The combined strengths of lithium-ion batteries enable the development of efficient energy storage systems that leverage their high energy density and reliability, as shown in Fig. 5. The DC bus and these storage units can be effectively managed using a bidirectional buck–boost converter. This converter facilitates power flow in both directions, allowing energy transfer from the DC bus to the battery during charging and from the battery to the load during discharging. Its capability to perform both step-down (buck) and step-up (boost) operations ensures proper voltage regulation under varying operating conditions. The converter plays a crucial role in maintaining stable DC bus voltage and controlling battery charging and discharging processes, thereby enhancing overall system performance and efficiency.

b. Operating Modes

The converter operates in two primary modes:

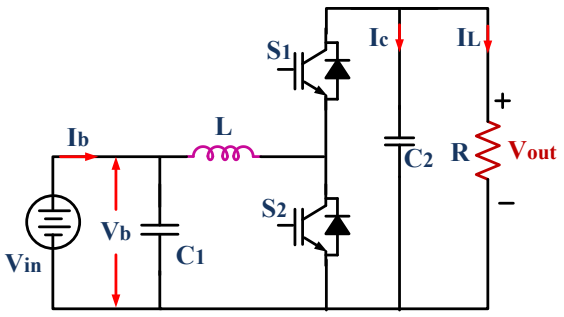

Fig.5 circuit diagram of DC-DC bidirectional buck boost converter

- **Buck Mode (Step-Down):** When the voltage on the DC bus is lower than the battery voltage (or supercapacitor voltage), the converter operates in buck mode to step down the voltage. This is typically used when discharging energy from the storage system to the bus or load.
- **Boost Mode (Step-Up):** When the voltage on the DC bus is higher than the storage voltage, the converter operates in boost mode to step up the voltage. This mode is used when charging the storage elements from the DC bus.

A single converter can operate in either mode by adjusting the duty cycle of its switching devices. In bidirectional operation, the power electronics (usually using MOSFETs or IGBTs) are arranged in an H-bridge or similar topology to allow current flow in both directions.

$$V_{out} = D \cdot V_{in} \quad (11)$$

Where: Vin is the input voltage (from the battery or DC bus), Vout is the regulated output voltage (to the load or storage device), D is the duty cycle, with 0<D<1.

c. Boost Mode (Step-Up Operation)

In boost mode, the converter increases the input voltage to a higher output voltage. The output voltage is expressed as:

$$V_{out} = \frac{V_{in}}{(1-D)} \quad (12)$$

Where: Vin is the lower voltage from the storage device or DC bus, Vout is the higher regulated voltage, D is the duty cycle, with 0<D<1.

d. Inductor and Capacitor Design

For both modes, an inductor L and output capacitor C are essential for smoothing the current and voltage ripples.

To ensure continuous conduction mode (CCM) and limit the inductor current ripple (ΔIL), the inductor value can be estimated by:

$$L = \frac{(V_{in} - V_{out}) \cdot D}{f_s - \Delta I_L} \quad (13)$$

$$L = \frac{V_{in} \cdot D}{f_s - \Delta I_L} \quad (14)$$

Where: f_s is the switching frequency, ΔI_L is the desired peak-to-peak inductor current ripple.

Capacitor Design

The output capacitor C smooths the voltage ripple (ΔV_{out}) at the output and is given by:

$$C = \frac{I_{out} \cdot D}{f_s - \Delta V_{out}} \quad (15)$$

Where: I_{out} is the load or charging current, ΔV_{out} is the acceptable output voltage ripple.

C. Modeling and Designing of Lithium-Ion Battery.

In modern power systems, Hybrid Energy Storage Systems (HESS) integrates multiple energy storage devices to enhance overall energy and power performance. Lithium-ion batteries, owing to their high energy density and efficiency, are widely utilized for sustained energy supply in such systems. The incorporation of multiple battery units facilitates improved operational flexibility and effective load management under varying conditions. This configuration enables enhanced load balancing, mitigates stress on individual battery units, and extends overall battery lifespan. Furthermore, it improves system responsiveness and reliability, making it highly suitable for applications such as electric vehicle (EV) charging, renewable energy integration, and microgrid operations.

a. Lithium-Ion Battery Modeling

The lithium-ion battery used in the proposed system is modeled using a nonlinear dynamic equation that captures both charging and discharging characteristics. The battery terminal voltage is expressed as:

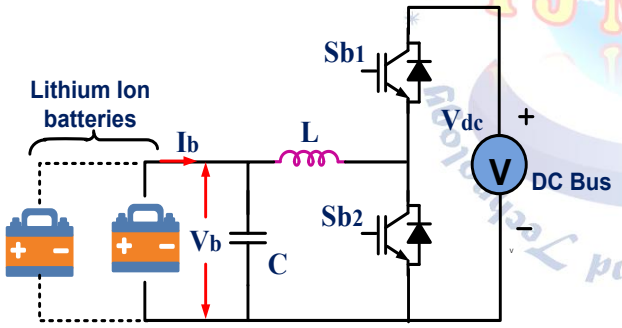

Fig.6 principle operation bidirectional dc-dc buck boost converter

$$E_B = E_0 - \frac{KQI_B}{Q - \int I_B\, dt} - K\frac{Q}{Q - \int I_B\, dt}\int I_B\, dt + A\exp(-B\int I_B\, dt) \quad (16)$$

where EB represents the battery terminal voltage, E0 is the constant open-circuit voltage, K denotes the polarization constant (V/Ah), Q is the maximum battery capacity (Ah), and IB is the battery current. The term ∫IB dt represents the extracted capacity over time. The exponential term Aexp(−B∫IBdt) models the voltage behavior in the exponential region of the battery discharge curve, where A and BBB are empirical constants. This model effectively captures the nonlinear voltage characteristics of lithium-ion batteries under varying load conditions. It accounts for polarization effects, capacity variation, and transient response during charging and discharging. The State of Charge (SoC) of the battery is estimated based on the integration of battery current, enabling accurate monitoring and control of energy storage units. The developed battery model is implemented for each BESS unit in the system, allowing decentralized control and SoC balancing across multiple batteries to enhance system reliability and lifespan.

b. Double-Loop Controller for EV Charging System

A double-loop control system is used as part of the control strategy for electric vehicle (EV) charging in order to guarantee safe, efficient, and reliable charging. The inner current loop controls the current going into the batteries, while the outside voltage loop keeps the DC bus voltage constant. To enhance dynamic performance and decrease steady-state error, a Proportional-Integral (PI) controller is used in both loops.

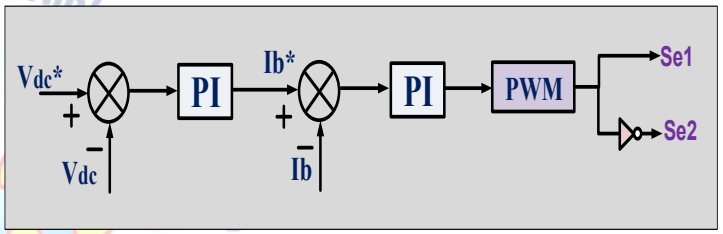

Fig. 7 double loop battery charging controller

1. Outer Voltage Loop: DC Bus Voltage Control

The outer voltage loop ensures the DC bus voltage (V_{dc}) remains stable and within the desired range. Since variations in EV charging loads and grid fluctuations affect the DC bus voltage, this loop provides a reference current (I_{ev}^*) for the inner current loop.

Error Signal Calculation:

$$e_v(t) = V_{dc}^* - V_{dc} \quad (17)$$

PI Controller Output (Reference EV Charging Current Iev∗)

$$I_{ev}^*(t) = K_{Pv}e_v(t) + k_{iv}\int e_v(t)\, dt \quad (18)$$

Where: Iev∗= Reference charging current for the inner loop, Kpv= Proportional gain of voltage controller, Kiv= Integral gain of voltage controller

This reference current is then passed to the inner current loop for precise battery charging control.

2. Inner Current Loop: Battery Current Control

To avoid overcharging and battery deterioration, the electric vehicle's inner current loop controls the charging current. Here, the PI controller determines the DC-DC converter's duty cycle, whether it's a buck or a boost.

Error Signal Calculation:

$$e_i(t) = I_{ev}^* - I_{ev} \quad (19)$$

PI Controller Output (Duty Cycle Control)

$$D(t) = K_{Pi} e_i(t) + k_{ii} \int e_i(t)\, dt \quad (20)$$

Where: D = Duty cycle of the DC-DC converter, Kpi= Proportional gain of current controller, Kii= Integral gain of current controller

This duty cycle (D) is applied to the DC-DC converter, adjusting the output voltage and current to regulate battery charging.

D. Working and Operation of the PMSG-Based Wind Energy Conversion System

The proposed wind energy conversion system consists of a wind turbine, a Permanent Magnet Synchronous Generator (PMSG), a three-phase diode rectifier, a boost converter, and a Maximum Power Point Tracking (MPPT) controller, as shown in Fig. 5. The primary objective of the system is to convert the available wind energy into regulated DC power and deliver it to the common DC bus of the EV charging station.

The wind turbine captures the kinetic energy available in the wind and converts it into mechanical power. The mechanical power extracted from the wind is given by

$$P_{wt} = \frac{1}{2} \rho A V_w^3 C_p(\lambda, \beta) \quad (21)$$

where Pwt is the wind turbine output power (W), ϱ is the air density (kg/m3), A is the swept area of the turbine blades (m2), Vw is the wind speed (m/s), and Cp is the power coefficient, which depends on the tip-speed ratio (λ) and blade pitch angle (β).

The tip-speed ratio is expressed as

$$\lambda = \frac{\omega_r R}{V_w} \quad (22)$$

where ωr is the rotor angular speed (rad/s) and R is the turbine blade radius (m).

The mechanical torque produced by the turbine is calculated as

$$T_m = \frac{P_{wt}}{\omega_r} \quad (23)$$

The generated mechanical power drives the Permanent Magnet Synchronous Generator (PMSG), which converts mechanical energy into three-phase electrical energy. The electrical output power of the PMSG can be expressed as

$$P_{PMSG} = T_e \cdot \omega_r \quad (24)$$

where Te is the electromagnetic torque of the generator.

The three-phase AC output of the PMSG is converted into DC voltage through the three-phase diode rectifier. The average output voltage of the rectifier is approximately

$$V_w = \frac{3\sqrt{2}}{\pi} V_{LL} \quad (25)$$

where VLL is the line-to-line RMS voltage of the PMSG.

The rectified voltage is filtered by the input capacitor Cin and supplied to the boost converter. The boost converter is employed to increase the rectified voltage and maintain the required DC-bus voltage. The output voltage of the boost converter is given by

$$V_{dc} = \frac{V_w}{1-D} \quad (26)$$

where:

- Vdc = DC-bus voltage (V)
- Vw = Rectified wind voltage (V)
- D = Duty cycle of the converter switch

The duty cycle is determined as

$$D = 1 - \frac{V_w}{V_{dc}} \quad (27)$$

The boost converter inductance is selected using

$$L = \frac{V_w \cdot D}{f_s \cdot \Delta I_L} \quad (28)$$

where fs is the switching frequency and ΔIL is the inductor current ripple.

Similarly, the output capacitor is calculated as

$$C = \frac{I_o \cdot D}{f_s \cdot \Delta V_{dc}} \quad (29)$$

where Io is the output current and ΔVdc is the allowable DC voltage ripple.

To maximize energy extraction, an MPPT controller continuously monitors the wind-side voltage and current and calculates the generated wind power as

$$P_w = V_w I_w \quad (30)$$

where Iw is the rectifier output current.

The MPPT controller adjusts the duty cycle of the boost converter switch according to wind speed variations so that the turbine operates at the optimum tip-speed ratio and maximum power point. As a result, the proposed PMSG-based wind energy conversion system efficiently converts variable wind energy into a regulated DC output, enhances renewable energy utilization, supports the DC bus, and reduces dependency on the utility grid in the fast EV charging station.

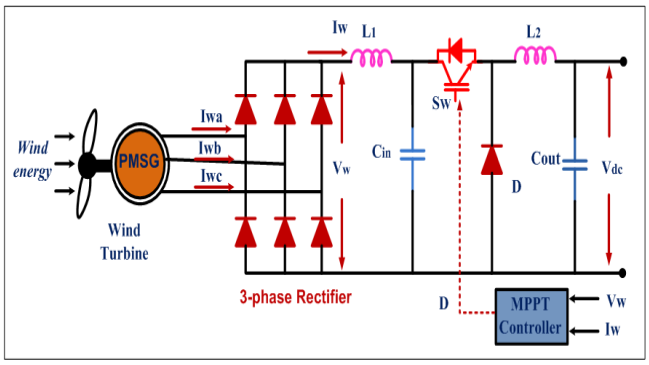

Fig.8 PMSG-based wind energy conversion topology with MPPT-controlled boost converter.

4. Proposed ANN Controller for VdcVoltage Regulation

To enhance the dynamic performance and adaptability of DC-link voltage regulation, an Artificial Neural Network (ANN)-based controller is employed. Unlike conventional controllers, the ANN can effectively handle nonlinearities, uncertainties, and varying operating conditions in hybrid PV–wind–BESS systems.

A. ANN Controller Structure

The ANN used in this work is a feed forward multilayer perceptron (MLP) consisting of an input layer, one hidden layer, and an output layer. The input variables to the ANN are selected as the DC-link voltage error and its rate of change:

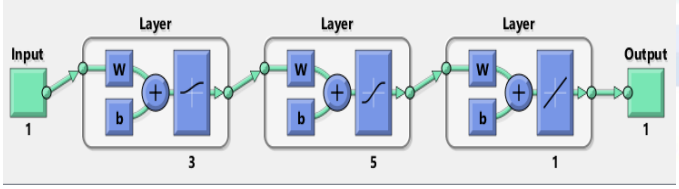

Fig 9: Structure of Neural Network

$$e(k) = V_{dc}^{*} - V_{dc}(k) \qquad (31)$$

$$\Delta e(k) = e(k) - e(k-1) \qquad (32)$$

where Vdc∗ is the reference DC-link voltage and Vdc(k) is the measured voltage at instant k.

The ANN output u(k) represents the control signal used to regulate the DC-link voltage through power converters.

$$h_j = f\left(\sum_{i=1}^{n} w_{ij}^{(1)} x_i + b_j^{(1)}\right) \qquad (33)$$

Where

xi = input variables (e,Δe),

wij(1) = weights between input and hidden layer,

bj(1) = bias of hidden neuron,

f(·) = activation function (typically sigmoid or ReLU).

The final ANN output is given by:

$$u(k) = \sum_{j=1}^{m} w_j^{(2)} h_j + b^{(2)} \qquad (34)$$

where

wj(2) = weights from hidden to output layer,

b(2) = output bias.

B. Training of ANN Controller

The ANN is trained using supervised learning to minimize the voltage regulation error. The cost function is defined as:

$$J = \frac{1}{2} e^2(k) \qquad (35)$$

The weights are updated using gradient descent (backpropagation):

$$w^{new} = w^{old} - \eta \frac{\partial J}{\partial w} \qquad (36)$$

where η is the learning rate.

Training data is generated from system simulations under different operating conditions, including variations in:

- PV irradiance
- Wind speed
- EV load demand
- BESS operating states

C. ANN-Based Control Strategy

The trained ANN generates the control signal u(k), which is used to regulate the DC-link voltage by adjusting the duty cycle of the DC–DC converter or modulation index of the converter. The control objective is to maintain:

$$V_{dc} \approx V_{dc}^{*} \qquad (37)$$

Under all operating conditions

5. Simulation Results and Discussion

The performance of the proposed Adaptive ANN-controlled DC-coupled fast EV charging station integrated with Wind–Solar Hybrid Energy Storage System (HESS) is evaluated under varying operating conditions. The simulation results analyze the dynamic behavior of grid voltage, grid current, wind generator current, battery current, and DC-bus voltage to verify the effectiveness of the proposed control strategy.

A. Grid Voltage Response

Fig. 10 shows the three-phase grid voltage waveform. It can be observed that the grid voltage remains balanced and sinusoidal throughout the simulation period. The voltage magnitude is maintained close to its rated value without noticeable distortion, demonstrating proper

synchronization between the grid-side converter and the utility grid. This confirms the effectiveness of the ANN-based controller in maintaining stable grid operation under varying load and renewable generation conditions.

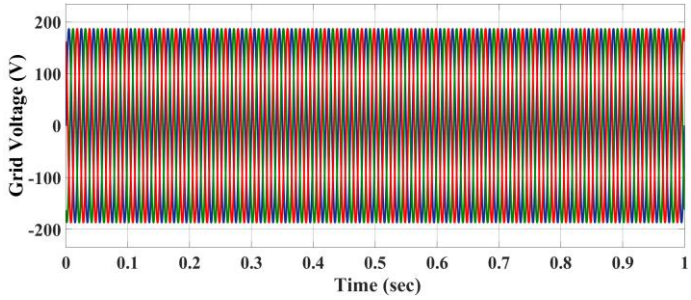

Fig.10 Three-Phase Grid Voltage Response

B. Grid Current Response

The three-phase grid current waveform is presented in Fig. 11. Initially, a higher current magnitude is observed due to increased charging demand and power exchange requirements. As the operating conditions change, the current magnitude decreases in a stepwise manner at approximately 0.2 s, 0.4 s, 0.6 s, and 0.8 s. These variations indicate dynamic power management between renewable sources, battery storage, and the utility grid. Despite these transitions, the current remains balanced and sinusoidal, confirming stable power transfer and effective current regulation.

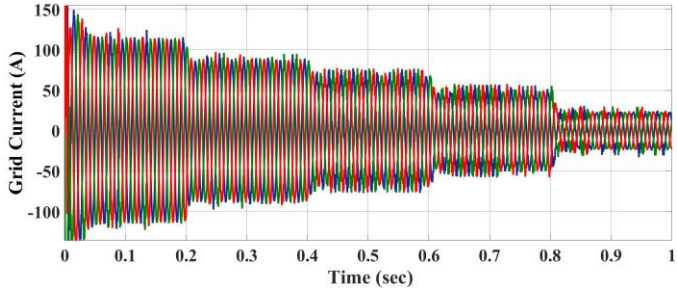

Fig.11 Three-Phase Grid Current Response

C. Wind Generator Current Response

Fig. 12 illustrates the wind generator current. The current initially operates at a higher magnitude and subsequently decreases around 0.4 s due to variations in wind power generation or power-sharing requirements. The smooth transition of the current waveform indicates proper operation of the wind energy conversion system and effective coordination by the ANN controller. The results confirm that the wind generation unit contributes significantly to the overall power demand while maintaining stable operation.

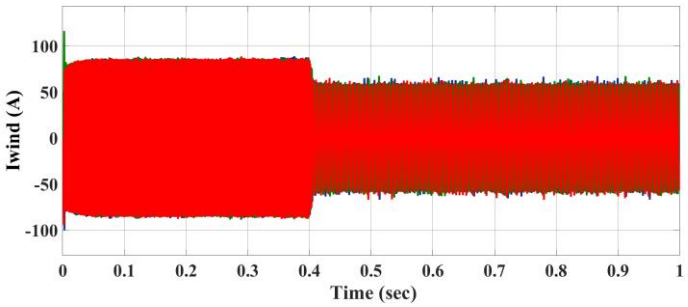

Fig.12 Wind Generator Current Response (Iwind)

D. Battery Current Response

The battery current response is shown in Fig.13. Negative current values indicate that the battery is operating in charging mode. Initially, the battery absorbs excess renewable energy with a charging current of approximately 80 A. As the system operating conditions change, the charging current gradually decreases, indicating controlled battery charging and energy management. The smooth current profile demonstrates the capability of the ANN controller to regulate battery charging power while maintaining system energy balance.

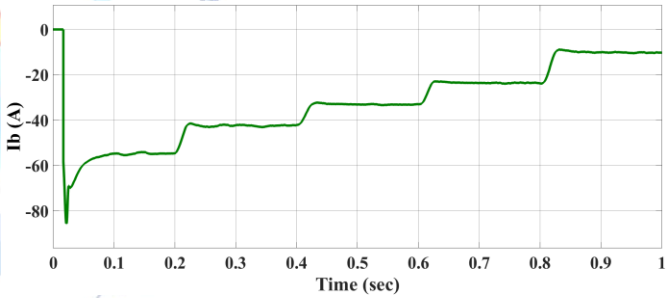

Fig.13 Battery Charging Current Response (Ib)

E. DC-Bus Voltage Regulation

Fig. 14 presents the DC-bus voltage response of the proposed charging station. During startup, a transient overshoot occurs due to converter initialization and capacitor charging. However, the voltage rapidly settles to approximately 400 V and remains stable throughout the simulation period. Small voltage variations observed during power transitions are effectively suppressed by the ANN controller. The stable DC-bus voltage confirms the ability of the proposed control strategy to maintain reliable operation of the EV charging station despite fluctuations in renewable generation and load demand.

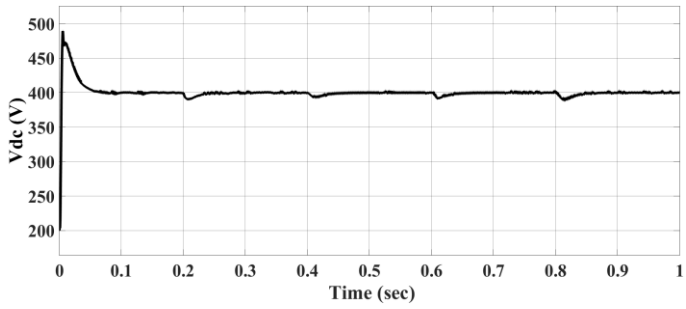

Fig.14 DC-Bus Voltage Response (Vdc)

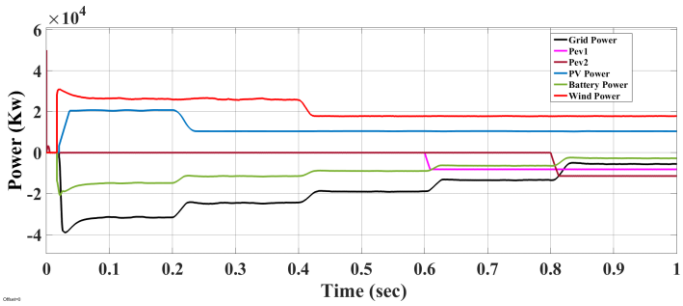

Fig. 15. Power-sharing performance of the proposed ANN-controlled EV charging station showing grid power, PV power, wind power, battery power, and EV load power.

F. Power Sharing Analysis

Fig. 15 illustrates the power-sharing performance of the proposed ANN-controlled DC-coupled fast EV charging station among the utility grid, PV system, wind generation system, battery energy storage system (BESS), and EV charging loads. The figure demonstrates the dynamic coordination of multiple energy sources under varying operating conditions. Initially, the PV array and wind energy conversion system provide a significant portion of the required power, while the battery absorbs excess renewable energy for storage. The grid power remains negative, indicating reduced dependency on the utility grid due to the contribution of renewable sources. Around 0.2 s and 0.4 s, changes in renewable generation result in corresponding adjustments in battery and grid power, demonstrating effective energy management and power balancing.

At approximately 0.6 s, the EV load demand changes, causing a redistribution of power among the available sources. The battery and renewable sources continue to support the load while maintaining stable system operation. Around 0.8 s, a further power transition occurs, and the grid contribution increases slightly to compensate for the reduction in renewable power availability. Throughout the simulation, the ANN controller effectively coordinates power flow among the PV system, wind generator, battery storage, EV loads, and utility grid. The results confirm that the proposed control strategy ensures optimal utilization of renewable energy, minimizes grid power consumption, maintains power balance, and enhances the overall reliability and efficiency of the fast EV charging station.

6. Conclusion

This paper presented an adaptive ANN-controlled DC-coupled fast EV charging station integrated with a wind–solar hybrid renewable energy system and battery energy storage system (BESS). The proposed architecture combines solar PV generation, wind energy conversion, battery storage, EV charging loads, and utility grid support through a common DC bus to achieve efficient energy management and reliable charging operation. An adaptive Artificial Neural Network (ANN)-based hierarchical control strategy was developed to regulate the DC-bus voltage and dynamically coordinate power flow among the available energy sources. Simulation results demonstrated that the proposed ANN controller effectively maintains DC-bus voltage stability, ensures balanced power sharing, and provides fast dynamic response under varying renewable generation and EV charging conditions. The integration of wind and solar energy improved renewable energy utilization and reduced dependence on the utility grid, while the battery storage system enhanced energy balancing and operational reliability. Furthermore, the proposed control strategy successfully managed power flow between the renewable sources, battery storage, EV loads, and grid, resulting in improved system stability and power quality. The obtained results confirm that the proposed ANN-controlled charging station outperforms conventional control approaches by providing superior adaptability, enhanced disturbance rejection capability, and efficient utilization of renewable energy resources. Therefore, the proposed system offers a robust, intelligent, and sustainable solution for next-generation fast EV charging infrastructure and smart grid applications.

Conflict of interest statement

Authors declare that they do not have any conflict of interest.

REFERENCES

[1] S. S. Refaat, O. Ellabban, S. Bayhan, H. Abu-Rub, F. Blaabjerg, and M. M. Begovic, Smart Grid and Enabling Technologies. Hoboken, NJ, USA: Wiley, 2021.

[2] I. S. Bayram, U. Zafar, and S. Bayhan, "Could petrol stations play a key role in transportation electrification? A GIS-based coverage maximization of fast EV chargers in urban environment," IEEE Access, vol. 10, pp. 17318–17329, 2022.

[3] Y. Zhang, J. Chen, L. Cai, and J. Pan, "Expanding EV charging networks considering transportation pattern and power supply limit," IEEE Trans. Smart Grid, vol. 10, no. 6, pp. 6332–6342, Nov. 2019.

[4] P. Chatterjee andM. Hermwille, "Tackling the challenges of electric vehicle fast charging," ATZelectronics Worldwide, vol. 15, no. 10, pp. 18–22, 2020.

[5] A. Sharida, S. Bayhan, and H. Abu-Rub, "Enhancing scalability of fast electric vehicle charging stations: Solutions for AC-DC side integration and regulation," IEEE Open J. Ind. Electron. Soc., vol. 4, pp. 720–731, 2023.

[6] F. Blaabjerg, H. Wang, I. Vernica, B. Liu, and P. Davari, "Reliability of power electronic systems for EV/HEV applications," Proc. IEEE, vol. 109, no. 6, pp. 1060–1076, Jun. 2021.

[7] H. Tu, H. Feng, S. Srdic, and S. Lukic, "Extreme fast charging of electric vehicles: A technology overview," IEEE Trans. Transp. Electrific., vol. 5, no. 4, pp. 861–878, Dec. 2019.

[8] N. Deb, R. Singh, R. R. Brooks, and K. Bai, "A review of extremely fast charging stations for electric vehicles," Energies, vol. 14, no. 22, 2021, Art. no. 7566.

[9] A. Verma, B. Singh, A. Chandra, and K. Al-Haddad, "An implementation of solar PV array based multifunctional EV charger," IEEE Trans. Ind. Appl., vol. 56, no. 4, pp. 4166–4178, Jul./Aug. 2020.

[10] M. Patterson, N. F. Macia, and A. M. Kannan, "Hybrid microgrid model based on solar photovoltaic battery fuel cell system for intermittent load applications," IEEE Trans. Energy Convers., vol. 30, no. 1, pp. 359–366, Mar. 2015.

[11] W. Vermeer, G. R. C. Mouli, and P. Bauer, "Optimal sizing and control of a PV-EV-BES charging system including primary frequency control and component degradation," IEEE Open J. Ind. Electron. Soc., vol. 3, pp. 236–251, 2022.

[12] N. Poursafar, S. Taghizadeh, M. J. Hossain, and M. Karimi-Ghartemani, "A voltage-supportive controller for ultra-fast electric vehicle chargers in islanded DC microgrids," J. Modern Power Syst. Clean Energy, vol. 11, no. 3, pp. 896–906, May 2023.

[13] F. Mandrile, D. Cittanti, V. Mallemaci, and R. Bojoi, "Electric vehicle ultra-fast battery chargers: A boost for power system stability?," World Elect. Veh. J., vol. 12, no. 1, 2021, Art. no. 16.

[14] I. Poonahela et al., "Hierarchical model-predictive droop control for voltage and frequency restoration in AC microgrids," IEEE Open J. Ind. Electron. Soc., vol. 4, pp. 85–97, 2023.

[15] Y. Dou, M. Chi, Z.-W. Liu, G. Wen, and Q. Sun, "Distributed secondary control for voltage regulation and optimal power sharing in DC microgrids," IEEE Trans. Control Syst. Technol., vol. 30, no. 6, pp. 2561–2572, Nov. 2022.

[16] A. Blanch-Fortuna, D. Zambrano-Prada, O. López-Santos, A. E. Aroudi, L. Vázquez-Seisdedos, and L. Martinez-Salamero, "Hierarchical control of power distribution in the hybrid energy storage system of an ultrafast charging station for electric vehicles," Energies, vol. 17, no. 6, 2024, Art. no. 1393.

[17] A. Sharida, N. Kamal, H. Alnuweiri, S. Bayhan, and H. Abu-Rub, "Digital twin-based diagnosis and tolerant control of t-type three-level rectifiers," IEEE Open J. Ind. Electron. Soc., vol. 4, pp. 230–241, 2023.

[18] M. H. Ibrahim, S. P. Ang, M. N. Dani, M. I. Rahman, R. Petra, and S. M. Sulthan, "Optimizing step-size of perturb & observe and incremental conductance MPPT techniques using PSO for grid-tied PV system," IEEE Access, vol. 11, pp. 13079–13090, 2023.

[19] S. Bayhan and H. Komurcugil, "Sliding-mode control strategy for threephase three-level T-type rectifiers with DC capacitor voltage balancing," IEEE Access, vol. 8, pp. 64555–64564, 2020.

[20] D. J. Rincon, M. A. Mantilla, J. M. Rey, M. Garnica, and D. Guilbert, "An overview of flexible current control strategies applied to LVRT capability for grid-connected inverters," Energies, vol. 16, no. 3, 2023, Art. no. 1052.